Journal of the Physical Society of Japan
Vol. 79, No. 12, December, 2010, 124713

Single Crystal Growth and Characterization of the Iron-Based Superconductor KFe_2As_2 Synthesized by KAs Flux Method

Kunihiro KIHOU[1,4*], Taku SAITO[2], Shigeyuki ISHIDA[3,4], Masamichi NAKAJIMA[3,4], Yasuhide TOMIOKA[1,4], Hideto FUKAZAWA[2,4], Yoh KOHORI[2,4], Toshimitsu ITO[1,4], Shin-ichi UCHIDA[3,4], Akira IYO[1,4], Chul-Ho LEE[1,4], and Hiroshi EISAKI[1,4]

[1]*National Institute of Advanced Industrial Science and Technology (AIST), Tsukuba, Ibaraki 305-8568, Japan*
[2]*Department of Physics, Chiba University, Chiba 263-8522, Japan*
[3]*Department of Physics, University of Tokyo, Bunkyo, Tokyo 113-0033, Japan*
[4]*Transformative Research-Project on Iron Pnictides (TRIP), JST, Chiyoda, Tokyo 102-0075, Japan*

(Received September 7, 2010; accepted October 4, 2010; published December 10, 2010)

Centimeter-sized platelet single crystals of KFe_2As_2 were grown using a self-flux method. An encapsulation technique using a commercial stainless steel container allowed the stable crystal growth to last for more than 2 weeks. Ternary K–Fe–As systems with various starting compositions were examined to determine the optimal growth conditions. The employment of KAs flux led to the growth of large single crystals with a typical size of as large as $15 \times 10 \times 0.4\,mm^3$. The grown crystals exhibit a sharp superconducting transition at 3.4 K with the transition width 0.2 K, as well as the very large residual resistivity ratio exceeding 450, evidencing the good sample quality.

KEYWORDS: Fe-based superconductor, KFe_2As_2, single crystal growth
DOI: 10.1143/JPSJ.79.124713

1. Introduction

Soon after the discovery of the superconductivity at 26 K in LaFeAs(O,F),[1] studies on the iron (Fe)-based superconductors have become one of the main research subjects in the field of material science. To date, a variety of superconductors, such as *Ln*FeAs(O,F) (*Ln*: rare earth), $(Ba,K)Fe_2As_2$, Fe(Se,Te), and LiFeAs, have been found and the superconducting critical temperature (T_c) exceeds 50 K, marking the highest record besides cuprates. Worldwide investigations towards developing novel high-T_c superconductors, as well as towards elucidating their superconducting mechanism, are now extensively in progress.[2]

Among various Fe-based superconductors, KFe_2As_2 stands out as a unique material. It is the end member of the $Ba_{1-x}K_xFe_2As_2$ solid solution system that exhibits the highest T_c of 38 K at $x = 0.4$.[3–5] Therefore, one can consider KFe_2As_2 as a "parent" compound, such as LaFeAsO or $BaFe_2As_2$, in that high-T_c superconductivity emerges upon its chemical substitution. However, while other parent compounds are all nonsuperconducting and exhibit a long-range antiferromagnetic order, KFe_2As_2 is a superconductor in itself, with a relatively low T_c of 3.8 K. The formal valence of Fe ions is 2.5+, much higher than those of other Fe-based superconductors, which are more or less 2+. As a result, the shape of the Fermi surface (FS) is expected to be significantly modified. Band structure calculations predict that while most of the Fe-based superconductors possess two-dimensional electron- and hole-FS sheets of roughly equal size, FSs of KFe_2As_2 are dominated by large hole sheets centered at the Γ point.[6] This feature is experimentally confirmed by angle-resolved photoemission spectroscopy (ARPES)[7] and de Hass–van Alphen (dHvA)[8] experiments. A different FS shape would lead the pairing interaction distinct from other Fe-based superconductors. Indeed, recent NMR,[9] penetration depth,[10] and thermal conductivity[11] measurements suggest that the superconducting gaps in KFe_2As_2 have nodes, in contrast to the nodeless gaps termed s± waves proposed for typical Fe-based superconductors,[12–17] such as $LnFeAsO_{1-x}F_x$, $(Ba,K)Fe_2As_2$, and $Ba(Fe,Co)_2As_2$. It is also interesting to note that the electronic specific heat is large,[9] suggesting a strong electron correlation and a large carrier mass, which is indeed confirmed by dHvA measurements.[8]

To sort out the intrinsic properties of materials, systematic investigations using sizable, high-quality single crystals are indispensable. In the case of $BaFe_2As_2$-related compounds, the flux method is commonly used to grow single crystals. There are a number of reports on the crystal growth of $(Ba,K)Fe_2As_2$ and $Ba(Fe,M)_2As_2$ (M = Co, Ni, Rh, Pd, Ru) by employing tin (Sn)[17–19] flux or FeAs[20–25] (self-) flux. As for KFe_2As_2, several groups have grown single crystals using FeAs flux.[11,26] The samples show superconducting transition at 3.0 K, slightly lower than the T_c of 3.8 K reported for polycrystalline samples. The in-plane residual resistivity ratio (RRR) of these crystals, defined by $\rho_{ab}(\sim 300\,K)/\rho_{ab}(4\,K)$, is estimated to be 86–87.

It is known that the single crystals grown using Sn flux contain several percent of Sn contamination, which markedly affects their physical properties. For example, in the case of $BaFe_2As_2$, Sn contamination results in the decrease in its structural/antiferromagnetic phase transition temperature from 138 to 80 K.[17] Accordingly, the self-flux method is more favorable in growing single crystals with better quality. Particularly, in the case of KFe_2As_2, crystal growth using FeAs self-flux is also expected to be difficult because of the difficulty in controlling potassium (K) at high temperatures. The vapor pressure of K increases at around the melting temperature of FeAs ($T_m = 1030\,^\circ C$), and in some cases, it attacks the sample container. As a result, a stable single crystal growth cannot be sustained, which should degrade the size and properties of the grown crystals.

*E-mail: k.kihou@aist.go.jp

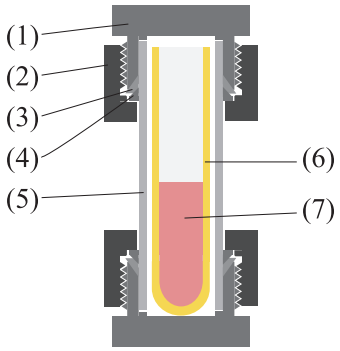

Fig. 1. (Color) Sealing assembly for the single crystal growth. (1) Cap union body (1-in. inner diameter), (2) cap union nut, (3) front ring, (4) back ring, (5) stainless tube (1-in. diameter), (6) alumina crucible, and (7) starting materials.

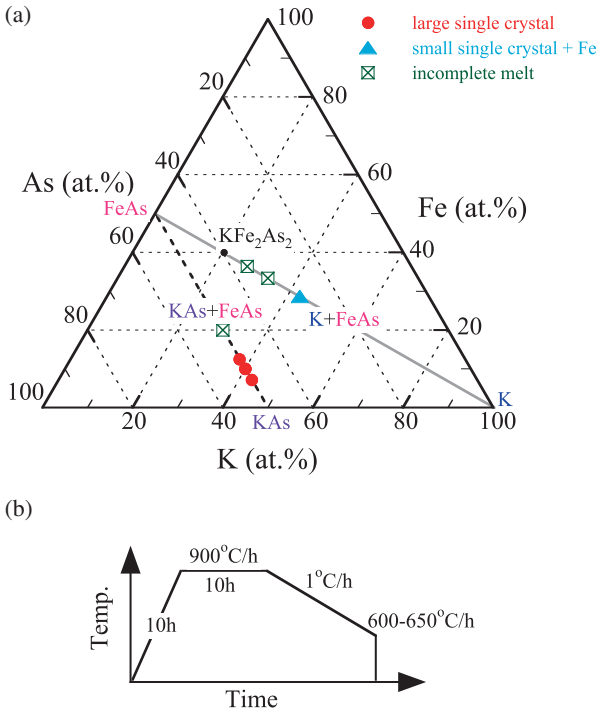

Fig. 2. (Color) (a) K–Fe–As triangular diagram for the compositions of the starting materials used to grow KFe_2As_2 single crystals. The compositions surveyed in the present study are indexed. (b) Temperature profile of the single crystal growth.

A possible solution to avoid such difficulty is to employ an adequate self-flux that allows the crystal growth at lower temperatures. Here, in this study, we have tested two kinds of self-flux with low T_m values, namely, K ($T_m = 63.7\,^\circ$C) and KAs ($T_m = 625\,^\circ$C), expecting that their lower T_m contributes to the stable synthesis of single crystal samples. Also, to prevent the corrosion between the sample container and the K vapor, we have developed an original encapsulation technique using a stainless steel sample container assembly. After some trials, we have found that the mixture of KAs and FeAs precursors with the mixing ratio KAs : FeAs = 3–6 : 1 is most effective in growing large single crystals with the typical size $15 \times 10 \times 0.4\,\text{mm}^3$. The crystals have a sharp superconducting transition at 3.5 K, and a large RRR exceeding 500, evidencing the good sample quality.

2. Experimental Methods

In this study, single crystals of KFe_2As_2 were grown using K-rich self-flux in a sealed environment. For the growth of $BaFe_2As_2$-related crystals, a quartz glass tube is usually used to seal the samples. However, this glass tube is not adequate in the present case since it suffers a significant chemical reaction with the evaporated K during the crystal growth. To avoid the reaction between the K vapor and the container, we have employed an encapsulation method using a commercial stainless steel container, as illustrated in Fig. 1. Here, an alumina crucible containing the starting materials is put in a steel tube. Tight sealing is accomplished by two caps also made of stainless steel, which are screwed to both ends of the tube. The container bears the temperature up to 1000 °C. The entire assembly can be obtained commercially.

The advantages of this encapsulation method are as follows. (1) Unlike a quartz tube, stainless steel does not react with K vapor. Accordingly, long-time crystal growth can be sustained. (2) The sealing process is simple and easy. In particular, welding is not required to seal the container. As a result, all preparation processes can be carried out inside the globe box, without exposing the reactive starting materials (K/KAs) in air. (3) The assembly used in this method is relatively cheaper than those used in other sealing methods.

The starting materials are K (3N, chunk), Fe (4N, 150 µm mesh), and As (6N, 1–5 mm chunk). In some cases, we used prereacted FeAs and KAs as starting materials. FeAs was synthesized by firing the mixture of Fe and As at 900 °C for 10 h in a sealed quartz tube. KAs was synthesized by firing the mixture of K and As at 650 °C for 10 h using a stainless steel container assembly.

Typically, 30 g of the mixture was put in an alumina crucible. Then, the alumina crucible was sealed in a stainless steel container. The process is carried out within a globe box filled with dried N_2. The humidity and oxygen content inside the globe box are kept below 1 ppm. The sample was placed in a box furnace and fired up to 900 °C for 10 h. The temperature was kept for 10 h, and then slowly cooled down to 600–650 °C at a cooling rate of 1 °C/h (lasting for 10 days), as shown in Fig. 2(b). After the crystal growth, flux was rinsed out of the samples using ethanol.

The composition of the grown single crystals was determined by energy-dispersive X-ray analysis with the scanning electron microscopy (SEM; JEOL JSM-6301F, EPMA; EDAX Phoenix 1M). The crystallinity of the single crystals was evaluated by X-ray Laue photography using a tungsten target. Lattice parameters were calculated using X-ray diffraction (XRD) patterns with Cu Kα radiation (Rigaku ULTIMA IV). Magnetic susceptibility was measured using a superconducting quantum interference device (SQUID) magnetometer (Quantum Design MPMS) under a magnetic field of 10 Oe. The dc resistivity was measured by a conventional four-probe method using Quantum Design PPMS.

3. Results and Discussion

3.1 Determination of the optimal growth composition

In Fig. 2(a), we summarize the compositions we have

examined to grow single crystals. The gray solid line corresponds to the solid solution of K and FeAs. Here, KFe_2As_2 is located on this line at K = 20 at. %. Along this line, K less than 20% corresponds to the FeAs self-flux growth condition and K more than 20% corresponds to the K self-flux growth condition. In this study, we employed the compositions K : FeAs = 1.5 : 2, 2 : 2, and 3 : 2, which are equal to K = 27, 33, and 43%, respectively. Among them, in the cases of K = 27 and 33%, melting was incomplete and the resultant material was a spongelike ingot with many voids. No single crystals were recognized. For K = 43%, a complete melting was accomplished and the resulting material was a dense ingot containing KFe_2As_2 single crystals with their typical dimensions less than $1 \times 1 \times 0.1$ mm^3. From the magnetic susceptibility and XRD measurements, the single crystals were found to contain ferromagnetic Fe impurities. These impurities were mainly located at the grain boundaries and could not be separated from the crystals. The most likely reason for the formation of Fe impurities is that a reaction, Liq. (K) + Solid (FeAs) → Liq. (K+As) + Solid (Fe), occurs while heating and the resultant Fe does not dissolve in the flux during the crystal growth.

To prevent any possible reaction, we then employed the flux containing a sufficient amount of K+As from the beginning. The dashed line in Fig. 2(a) represents the solid solution of FeAs and KAs. In this study, we examined the mixture of KAs and FeAs with the molar ratio 1.5 : 1, 3 : 1, 4 : 1, and 6 : 1, which corresponds to the K concentration of 30, 38, 40, and 43%, respectively. Among them, the K concentrations larger than 38% yielded a complete melting. KFe_2As_2 single crystals can be found inside the grown ingot. The size of the crystals increases with increasing KAs flux concentration, reaching $15 \times 10 \times 0.4\,mm^3$ in the case of KAs : FeAs = 6 : 1. The photograph of the grown crystal is shown in Fig. 3(a) together with a millimeter scale. SQUID and XRD measurements indicate that the grown crystals are free from Fe impurities. We therefore used these crystals for the characterization and the physical property measurements.

3.2 *Crystallographic characterization*

As seen in Fig. 3(a), the grown crystals exhibit a platelike morphology with flat, shinny, black surfaces. The sample easily cleaves along these surfaces. An X-ray Laue backscattering photograph from the cleaved surface is shown in Fig. 3(b). A fourfold symmetry is easily recognized, indicating that the flat surface corresponds to the (001) plane of the tetragonal KFe_2As_2 unit cell. Figure 3(c) shows the X-ray diffraction pattern with the (00*l*) reflections. The *c*-axis lattice constant $c = 13.88$ Å calculated from the observed peaks is consistent with the literature value reported for the polycrystalline samples.[3)]

According to the microprobe analysis, the composition of the grown crystal is estimated as K : Fe : As = 20.84 : 37.57 : 41.59, in accordance with the stoichiometric composition of 1 : 2 : 2 within the experimental accuracy. The result suggests that there is no appreciable K deficiency in our single crystals.

In Figs. 4(a) and 4(b), we show the SEM micrographs of the single crystal. As seen in Fig. 4(a), the crystal exhibits a

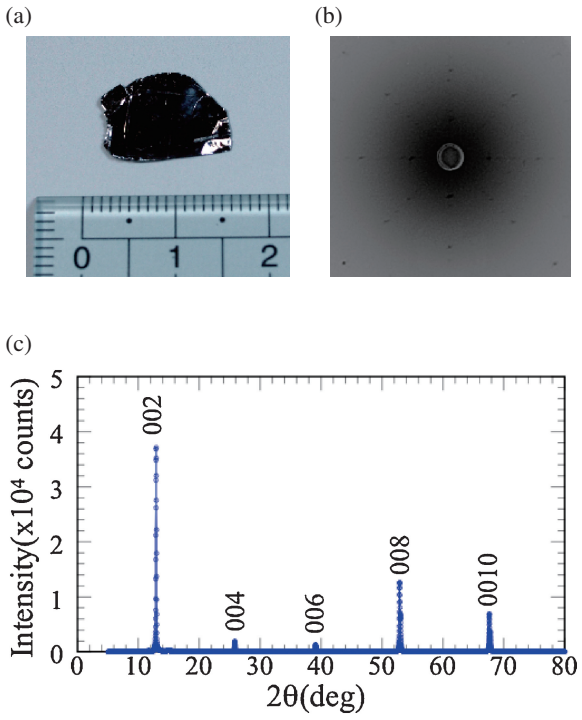

Fig. 3. (Color) (a) Photograph of the KFe_2As_2 single crystal together with a millimeter scale. (b) Back-reflected Laue photograph of KFe_2As_2. The incident X-ray beam was applied normal to the cleaved surface. (c) X-ray diffraction pattern of the KFe_2As_2 single crystal. Only (00*l*) peaks are recognized.

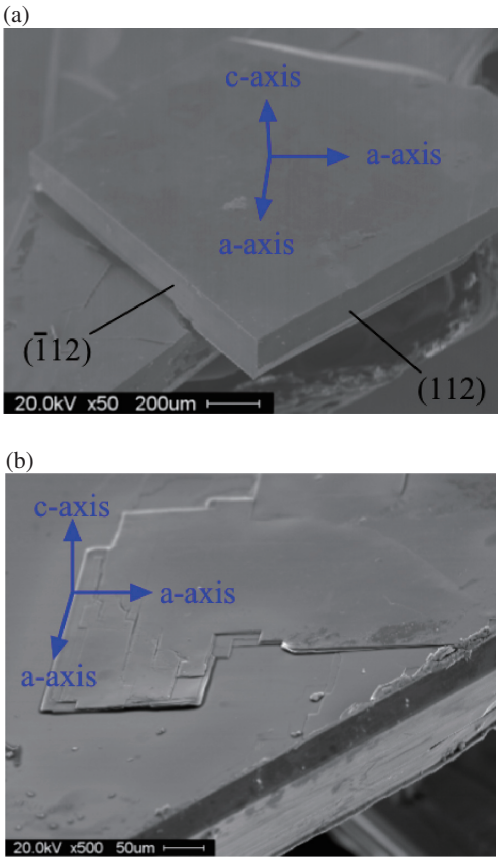

Fig. 4. (Color) SEM micrographs of KFe_2As_2. (a) Typical single crystal possessing well-developed facets. (b) (001) face after the cleavage. Multilayer stacks with edges arraying along the [100] direction are recognized.

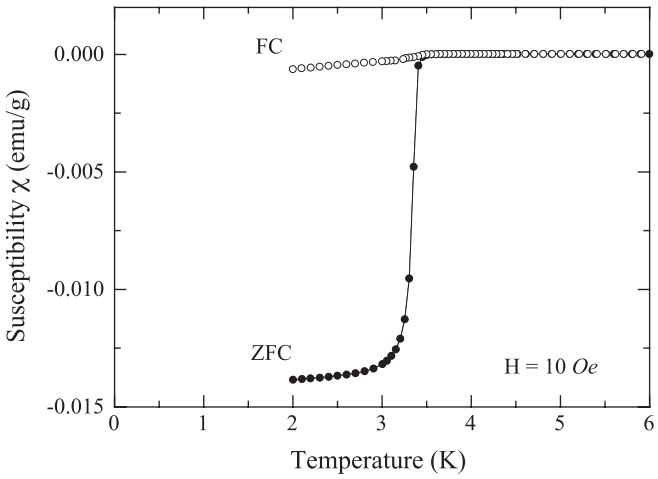

Fig. 5. Temperature dependence of the magnetic susceptibility for the KFe_2As_2 single crystal. Measurement was carried out under the magnetic field of 10 Oe applied perpendicularly to the *c*-axis.

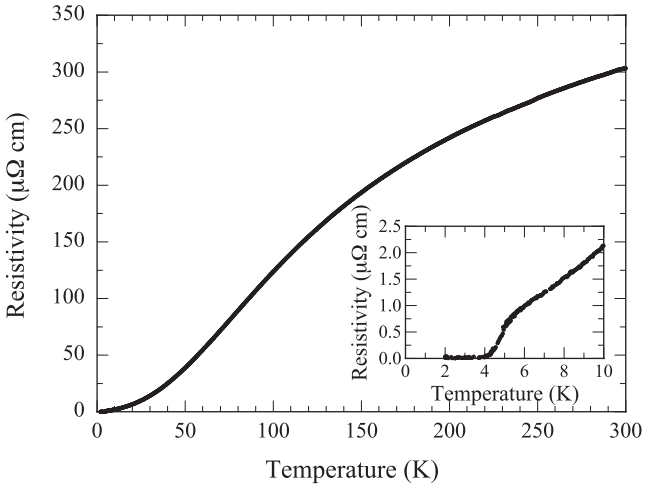

Fig. 6. Temperature dependence of the in-plane dc resistivity for the KFe_2As_2 single crystal. The inset shows the same data around the superconducting transition.

tetragonal shape, reflecting the layered, tetragonal crystal structure of KFe_2As_2. The large plane corresponds to the (001) face and the edges of the crystals are identified as (112) facets, which are running along the [110] crystallization axis.

On the (001) face, one can recognize terrace structures comprised of multiple layers with a thickness of 5 μm [Fig. 4(b)]. The terrace is formed upon the cleavage of the surface layer. The figures show that KFe_2As_2 selectively cleaves along the [100] direction (besides the [001] direction), 45° off the growth facets running along the [110] axis.

3.3 Physical properties

Figure 5 shows the temperature dependences of the zero-field-cooling (ZFC) and field-cooling (FC) magnetic susceptibilities (χ) under the magnetic field of 10 Oe applied perpendicularly to the *c*-axis. Both ZFC and ZF curves show a well-defined drop at 3.4 K, indicative of the onset of superconducting transition at this temperature. The 10–90% transition width is as small as 0.2 K. The T_c value and superconducting transition width of the present sample are superior to those reported in the literature.[11,26] The volume fraction estimated from the ZFC value below 3 K is approximately 100%, indicating the bulk nature of the superconductivity. The sharp superconducting transition, higher T_c, and large volume fraction signify the good quality of the present samples. We also note that T_c is precisely reproducible. There is no appreciable difference in T_c (within 0.2 K) among the grown samples. The signal above T_c is nearly zero, indicating that the sample is free from magnetic impurities.

Figure 6 shows the typical in-plane dc resistivity [$\rho_{ab}(T)$] of the grown crystal. The resistivity shows metallic ($d\rho_{ab}/dT > 0$) behavior in the entire temperature range. The RRR, which is defined by $\rho_{ab}(300\,K)/\rho_{ab}(5\,K)$, is as large as 458, indicating that the present sample is extremely clean, almost free from elastic impurity scattering. The number is much larger than the value of 87–88 reported on the crystals grown by the FeAs flux method.[11,26] The low-temperature ($T < 30$ K) resistivity follows the Fermi-liquid dependence, namely, $\rho_{ab}(T) = \rho_0 + AT^2$. Its physical implication is depicted in refs. 9 and 10.

The electrical resistivity has decreased gradually at around 3.8 K. T_c(midpoint) = 3.5 K, and T_c(zero resistivity) = 3.4 K, respectively. The T_c determined by the zero resistivity is consistent with the onset of a diamagnetic signal. Accordingly, we employ the $T_c = 3.4$ K defined by the magnetic susceptibility as the bulk T_c of the obtained single crystals.

4. Conclusions

We have successfully grown centimeter-sized platelet single crystals of KFe_2As_2 using a self-flux method. An encapsulation technique using a stainless steel container was developed, which allowed the stable crystal growth to last for more than 2 weeks. Ternary K–Fe–As systems with various starting compositions were examined to establish the optimal growth conditions. The employment of KAs flux led to the growth of large single crystals with a typical size of as large as $15 \times 10 \times 0.4\,mm^3$. The grown crystals exhibit a sharp superconducting transition at 3.4 K with the transition width 0.2 K as well as the residual resistivity ratio exceeding 450, evidencing the good sample quality.

Acknowledgements

The authors thank P. M. Shirage, H. Kito, Y. Yoshida, M. Ishikado, T. Terashima, M. Kimata, S. Uji, T. Yoshida, A. Fujimori, K. Hashimoto, T. Shibauchi, Y. Matsuda, and H. Kawano-Furukawa for valuable discussions and K. Shimada for SEM measurements. This work was supported by Grants-in-Aid for Specially Promoted Research (20001004) and for Scientific Research on Innovative Areas "Heavy Electrons" (No. 20102005) from the Ministry of Education, Culture, Sports, Science and Technology of Japan and by a Grant-in-Aid for Scientific Research C (No. 22540380) from the Japan Society for the Promotion of Science and by Mitsubishi Foundation.

1) Y. Kamihara, T. Watanabe, M. Hirano, and H. Hosono: J. Am. Chem. Soc. **130** (2008) 3296.
2) K. Ishida, Y. Nakai, and H. Hosono: J. Phys. Soc. Jpn. **78** (2009) 062001.
3) M. Rotter, M. Pangerl, M. Tegel, and D. Johrendt: Angew. Chem., Int. Ed. **47** (2008) 7949.
4) H. Chen, Y. Ren, Y. Qiu, W. Bao, R. H. Liu, G. Wu, T. Wu, Y. L. Xie, X. F. Wang, Q. Huang, and X. H. Chen: Europhys. Lett. **85** (2009) 17006.
5) K. Sasmal, B. Lv. B. Lorfenz, A. M. Guloy, F. Chen, Y.-Y. Xue, and C.-W. Chu: Phys. Rev. Lett. **101** (2008) 107007.
6) D. J. Singh: Phys. Rev. B **79** (2009) 174520.
7) T. Sato, K. Nakayama, Y. Sekiba, P. Richard, Y.-M. Xu, S. Souma, T. Takahashi, G. F. Chen, J. L. Luo, N. L. Wang, and H. Ding: Phys. Rev. Lett. **103** (2009) 047002.
8) T. Terashima, M. Kimata, N. Kurita, H. Satsukawa, A. Harada, K. Hazama, M. Imai, A. Sato, K. Kihou, C. H. Lee, H. Kito, H. Eisaki, A. Iyo, T. Saito, H. Fukazawa, Y. Kohori, H. Harima, and S. Uji: J. Phys. Soc. Jpn. **79** (2010) 053702.
9) H. Fukazawa, Y. Yamada, K. Kondo, T. Saito, Y. Kohori, K. Kuga, Y. Matsumoto, S. Nakatsuji, H. Kito, P. M. Shirage, K. Kihou, N. Takeshita, C. H. Lee, A. Iyo, and H. Eisaki: J. Phys. Soc. Jpn. **78** (2009) 083712.
10) K. Hashimoto, A. Serafin, S. Tonegawa, R. Katsumata, R. Okazaki, T. Saito, H. Fukazawa, Y. Kohori, K. Kihou, C. H. Lee, A. Iyo, H. Eisaki, H. Ikeda, Y. Matsuda, A. Carrington, and T. Shibauchi: Phys. Rev. B **82** (2010) 014526.
11) J. K. Dong, S. Y. Zhou, T. Y. Guan, H. Zhang, Y. F. Dai, X. Qiu, X. F. Wang, Y. He, X. H. Chen, and S. Y. Li: Phys. Rev. Lett. **104** (2010) 087005.
12) K. Hashimoto, T. Shibauchi, T. Kato, K. Ikada, R. Okazaki, H. Shishido, M. Ishikado, H. Kito, A. Iyo, H. Eisaki, S. Shamoto, and Y. Matsuda: Phys. Rev. Lett. **102** (2009) 017002.
13) K. Hashimoto, T. Shibauchi, S. Kasahara, K. Ikada, S. Tonegawa, T. Kato, R. Okazaki, C. J. van der Beek, M. Konczykowski, H. Takeya, K. Hirata, T. Terashima, and Y. Matsuda: Phys. Rev. Lett. **102** (2009) 207001.
14) L. Malone, J. D. Fletcher, A. Serafin, A. Carrington, N. D. Zhigadlo, Z. Bukowski, S. Katrych, and J. Karpinski: Phys. Rev. B **79** (2009) 140501(R).
15) H. Ding, P. Richard, K. Nakayama, K. Sugawara, T. Arakane, Y. Sekiba, A. Takayama, S. Souma, T. Sato, T. Takahashi, Z. Wang, X. Dai, Z. Fang, G. F. Chen, J. L. Luo, and N. L. Wang: Europhys. Lett. **83** (2008) 47001.
16) H. Kim, R. T. Gordon, M. A. Tanatar, J. Hua, U. Welp, W. K. Kwok, N. Ni, S. L. Bud'ko, P. C. Canfield, A. B. Vorontsov, and R. Prozorov: Phys. Rev. B **82** (2010) 060518(R).
17) N. Ni, S. L. Bud'ko, A. Kreyssig, S. Nandi, G. E. Rustan, A. I. Goldman, S. Gupta, J. D. Corbett, A. Kracher, and P. C. Canfield: Phys. Rev. B **78** (2008) 014507.
18) J. S. Kim, E. G. Kim, and G. R. Stewart: J. Phys.: Condens. Matter. **21** (2009) 252201.
19) P. Reuvekamp, F. S. Razavi, C. Hoch, J. S. Kim, R. K. Kremer, and A. Simon: J. Supercond. Novel Magn. **22** (2009) 353.
20) H. Luo, Z. Wang, H. Yang, P. Cheng, X. Zhu, and H. Wen: Supercond. Sci. Technol. **21** (2008) 125014.
21) N. Ni, M. E. Tillman, J.-Q. Yan, A. Kracher, S. T. Hannahs, S. L. Bud'ko, and P. C. Canfield: Phys. Rev. B **78** (2008) 214515.
22) X. F. Wang, T. Wu, G. Wu, H. Chen, Y. L. Xie, J. J. Ying, Y. J. Yan, R. H. Liu, and X. H. Chen: Phys. Rev. Lett. **102** (2009) 117005.
23) N. Ni, A. Thaler, A. Kracher, J. Q. Yan, S. L. Bud'ko, and P. C. Canfield: Phys. Rev. B **80** (2009) 024511.
24) R. Morinaga, K. Matan, H. S. Suzuki, and T. J. Sato: Jpn. J. Appl. Phys. **48** (2009) 013004.
25) A. S. Sefat, D. J. Singh, R. Jin, M. A. McGuire, B. C. Sales, F. Ronning, and D. Mandrus: Physica C **469** (2009) 350.
26) T. Terashima, M. Kimata, H. Satsukawa, A. Harada, K. Hazama, S. Uji, H. Harima, G.-F. Chen, J.-L. Luo, and N.-L. Wang: J. Phys. Soc. Jpn. **78** (2009) 063702.